PHYSICAL REVIEW C, VOLUME 61, 041601(R)

Unexpected transparency in low energy ^{90}Zr(α,α_0) scattering and α-cluster structure in ^{94}Mo

F. Michel,[1] G. Reidemeister,[2] and S. Ohkubo[3]
[1]*Faculté des Sciences, Université de Mons-Hainaut, B-7000 Mons, Belgium*
[2]*Faculté des Sciences, Université Libre de Bruxelles, CP229, B-1050 Bruxelles, Belgium*
[3]*Department of Applied Science and Environment, Kochi Women's University, Kochi 780-8515, Japan*
(Received 13 January 2000; published 15 March 2000)

We show that incomplete absorption in ^{90}Zr(α,α_0) scattering is responsible for the spectacular dip observed in the backward excitation function at low energy ($E_\alpha \simeq$ 25 MeV), which we interpret as a destructive interference effect between the barrier and internal wave contributions to the scattering amplitude. Because of this transparency, an optical potential, which is in line with the higher energy data, can be extracted with good accuracy. The real part of this potential is found to support several rotational bands; the properties of the states of the first Pauli-allowed band, with $N=16$, in particular the electromagnetic transition rates between the first states, are in good agreement with those of the states of the experimental ^{94}Mo ground state band, suggesting that α-cluster structure is still an important feature in the $A=90$ region.

PACS number(s): 21.60.Gx, 24.10.Ht, 25.55.Ci, 27.60.+j

α-cluster structure is a dominant and unmistakable feature of the spectroscopy of light nuclei. In particular, many intruder states appearing in the low energy spectra of these nuclei can be understood in a simple and pictorial way in terms of α-particle clustering [1]. Whether this concept can be usefully extended to heavier mass nuclei is a matter of great interest [2,3] and has been a key issue in several recent papers [4–6]. In this Rapid Communication, we present new arguments in favor of the persistence of alpha-cluster structure in the $A=90$ mass region.

α clustering is now known to persist at least up to the sd-shell closure and the beginning of the fp shell [7,8]. For example, the ground state band in ^{44}Ti, which is the fp-shell analog of the ^{20}Ne ground state band—whose description in terms of α-cluster structure is well established [1]—can, like the latter, be understood in terms of an α particle orbiting an unexcited closed-shell core. This interpretation was first put forward on the basis of local potential model (LPM) calculations [9,10], similar to those performed earlier by Buck, Dover, and Vary [11] for investigating α-cluster structure in ^{20}Ne. This picture was considerably reinforced in a subsequent study [7,12], where the real part of a unique global optical model (OM) potential, fitting the ^{40}Ca(α,α_0) differential cross sections down to about 20 MeV incident energy, was shown to automatically locate the states of the ^{44}Ti ground state band at the correct absolute energy, with electromagnetic properties in good agreement with experiment.

The validity of the (seemingly simplistic) LPM approach is now well understood in more microscopic terms. In particular, the local potential equivalent to the strongly nonlocal resonating group method (RGM) interaction was shown [13] to depend weakly on angular momentum and to be deep; this potential supports a number of bound states, which have the same quantum numbers as the so-called forbidden states of the RGM, and which have thus to be discarded, while bound, quasibound, and scattering states with higher quantum numbers are physically allowed. In the LPM calculation of Refs. [7,12], bound states with a principal quantum number $N=2n+l$ less than 12, which correspond to the RGM forbidden states for the $\alpha+^{40}$Ca system, were discarded; the states of the ^{44}Ti ground state band, with even spins ranging from 0 to 12, correspond in this interpretation to the allowed states with $N=12$ [7,12,14–16]. An extension of the LPM approach to several nuclei of the sd-shell closure region suggested that α-clustering could be an important ingredient for understanding the low energy nuclear properties in this mass region [17]. A recent account of the present status of α clustering in medium-weight nuclei can be found in Ref. [3].

Because of strong absorption, the OM potential is rarely determined precisely on the whole radial range, especially if use is made of data extending on a restricted angular range. However, it has been shown that the OM potential can be traced with good accuracy down to low energies, provided absorption is mild enough to allow part of the incident flux, which passes the Coulomb barrier and penetrates the nuclear interior, to survive the scattering in the elastic channel and to bring back information on the α-nucleus interaction at much smaller distances than usual; if this ''internal'' information is missing, which is the case if absorption is strong and/or if the data are restricted to too small an angular range, the OM potential can be determined only beyond the barrier radius, around the so-called strong absorption radius. This admittedly rather exceptional situation—which has been termed incomplete absorption [18]—has up to now been encountered for several targets around the p- and the sd-shell closures [8]; in these cases, the internal contribution to the scattering manifests itself at large angles as an anomalous enhancement of the elastic cross section, which is then dominated at these angles by the internal contribution to the elastic scattering amplitude [19].

One of the aims of this Rapid Communication is to prove that incomplete absorption, which had up to now not been mentioned for α-particle scattering from nuclei heavier than about $A=40$, persists in fact at least up to the $A=90$ region. Several optical model or coupled channel studies have been devoted to the $\alpha+^{90}$Zr interaction [20–22]; more recently, LPM (and in particular folding model) calculations have been reported for the $\alpha+^{90}$Zr system, both in the scattering and in the bound state energy regions [4–6]. While the LPM calculations of Buck *et al.* [4], which make use of a modified

Woods-Saxon potential, are restricted to the bound and quasibound state properties of the $\alpha+{}^{90}\mathrm{Zr}={}^{94}\mathrm{Mo}$ system, the double folding model potentials of Ohkubo [5] and of Atzrott *et al.* [6], used for predicting the low energy properties of ^{94}Mo, were tested against the $\alpha+{}^{90}$Zr elastic scattering data in a broad range of energies and angles. Although Kobos *et al.* [22], in their folding model analysis, interpret the existence of two maxima in the Airy rainbow pattern at 79.5 MeV in terms of a particular transparency of the potential at this energy, and the error band on the real part of the potential at 40 and 118 MeV is briefly discussed in Ref. [6], none of these studies addresses the problem of the possible existence of an internal wave contribution to the scattering amplitude at low energy, and thus that of the sensitivity of the low energy scattering cross section to the potential at small distances.

We found that the most convincing evidence for the existence of such a sensitivity is contained in $^{90}\mathrm{Zr}(\alpha,\alpha_0)$ data of Wit *et al.* [23], which have to this date remained largely unnoticed. This group measured α-particle elastic scattering excitation functions, and angular distributions extending on the whole angular range between 18 and 26 MeV, for several nuclei around $A=90$. The most spectacular and unexpected feature of these data is the appearance of a narrow ($\Delta E \simeq 0.5$ MeV) and deep dip in the excitation functions near 180° for the ^{89}Y and ^{90,91}Zr targets around 23 MeV incident energy. This dip is correlated with a deep minimum in the differential cross section around 180°, a rare phenomenon since a maximum is observed at this angle for the vast majority of the available α + nucleus angular distributions; at neighboring energies a more classic maximum is indeed observed in $^{90}\mathrm{Zr}(\alpha,\alpha_0)$. Wit *et al.* [23] succeeded in reproducing qualitatively their data within an optical model approach, using a simple four-parameter Woods-Saxon potential, but a full understanding of the phenomenon was evidently not attained. It was shown incidentally by Albiński and Michel [24] that this deep minimum results from an accidental destructive interference between the internal and barrier wave contributions to the scattering amplitude at this energy and angle; however, in the absence of additional physical motivation this point was not investigated further.

In the present work, we first reinvestigated the properties of the optical potential which describes the low energy $^{90}\mathrm{Zr}(\alpha,\alpha_0)$ data, especially since the potential used by Wit *et al.* [23] has serious deficiencies in the small angle region at 23.4 and 25 MeV, where the calculated angular distribututions are out of phase with the data. (In Ref. [23] the authors found it impossible to remedy this defect without losing the good description of the backangle phenomenon.) Moreover, we insisted on reproducing the low energy anomaly using a potential which is in line with those describing higher energy data, in particular at the next energy where a complete angular distribution is available, that is, 40 MeV. Finally, we searched for a potential belonging to the unique potential family which describes the data above about 100 MeV; the volume integral per nucleon pair j_V of the real part of this potential is about 300 MeV fm^3 at 141.7 MeV [21]. Use was made of the same form factors as those used in the successful global optical model analysis [25] of the $^{16}\mathrm{O}(\alpha,\alpha_0)$ data—which offer one of the most remarkable cases of incomplete absorption at low energy—between 16 and 160 MeV, that is

$$V(r) = -V_0\{1+\alpha\exp[-(r/\rho)^2]\}/\{1+\exp[(r-R_V)/2a_V]\}^2 + V_C(r),$$

$$W(r) = -W_0/\{1+\exp[(r-R_W)/2a_W]\}^2, \qquad (1)$$

for the real and imaginary parts of the potential, respectively. The form factor used for the real part has more parameters than the conventional Woods-Saxon or Woods-Saxon squared form factors; however, in the $\alpha+{}^{16}$O case, this additional flexibility made possible the reproduction of the complicated energy dependence of the data with a fixed set of parameters for the real part of the potential, except for α, which was used to control the real potential strength and found to vary smoothly on the whole energy range [25].

An excellent agreement with the data at 25 and 40 MeV was obtained within this scheme, resulting in the parameter values $V_0=35$ MeV, $R_V=7.56$ fm, $a_V=0.43$ fm, and $\rho=4.93$ fm; the imaginary potential parameters were adjusted independently at the two energies. The energy dependent parameters α, W_0, R_W, and a_W take the values 4.748, 17.5 MeV, 6.52 fm, and 0.135 fm, respectively, at 25 MeV, and 4.801, 15.2 MeV, 7.44 fm, and 0.251 fm, respectively, at 40 MeV. These correspond to real volume integrals per nucleon pair $j_V=346$ and 348 MeV fm^3 at 25 and 40 MeV, respectively.

The parameters obtained at 25 MeV automatically describe the 21 and 23.4 MeV data in a very satisfactory way, including the dip around 180° at 23.4 MeV, as can be seen in Fig. 1 where the data between 21 and 40 MeV are compared with the OM calculations; it can be concluded from the good agreement at 21, 23.4, and 25 MeV that the small angle problem encountered by Wit *et al.* [23] was due to the use of an inadequate form factor. We also note that the small discrepancy observed at 40 MeV around $\theta=100°$ can easily be corrected by adding a small surface term in the absorptive potential; since this small modification does not affect the conclusions of the forthcoming discussion we will in the following stick to the above version of the potential.

A comparison of the experimental excitation function at 176° between 18 and 26 MeV with the predictions of the 25 MeV potential appears in Fig. 2(a); it is seen that the spectacular dip around 23.5 MeV is accurately reproduced by the calculation. To understand the origin of this dip, it is instructive to decompose the elastic scattering amplitude $f(\theta)$ into its barrier and internal wave contributions, $f_B(\theta)$ and $f_I(\theta)$, as defined within a semiclassical context by Brink and Takigawa [19]. It was shown by Albiński and Michel [24] that this decomposition can be performed in a fully quantum way by repeating several optical model calculations using slightly modified versions of the imaginary part of the optical potential in the internal region, that is, inside of the barrier radius at the grazing angular momentum. We have performed such a decomposition at 21, 23.4, and 25 MeV (see Fig. 3); it is seen that while the barrier contribution dominates the scat-

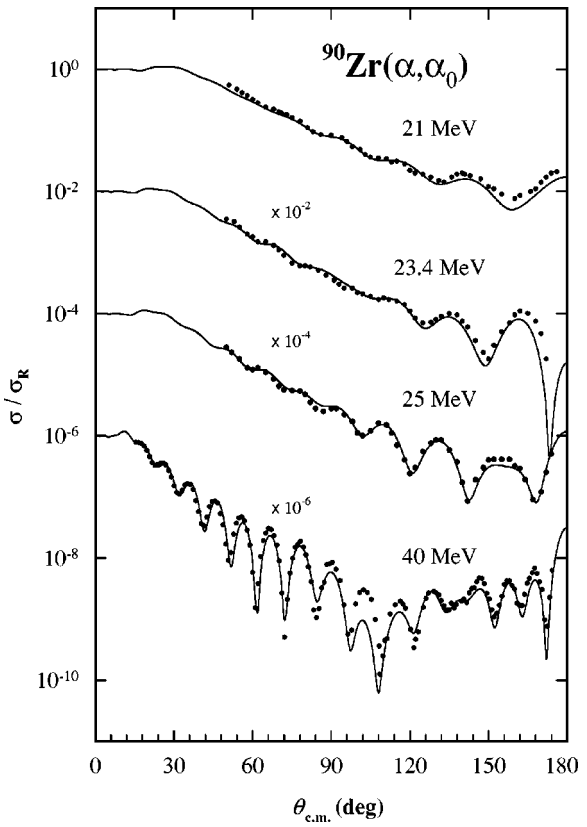

FIG. 1. Comparison of the experimental $^{90}\mathrm{Zr}(\alpha,\alpha_0)$ angular distributions at 21, 23.4, and 25 MeV [23] and at 40 MeV [21], with the predictions of the optical potential. The potential parameters at 21 and 23.4 MeV are the same as at 25 MeV.

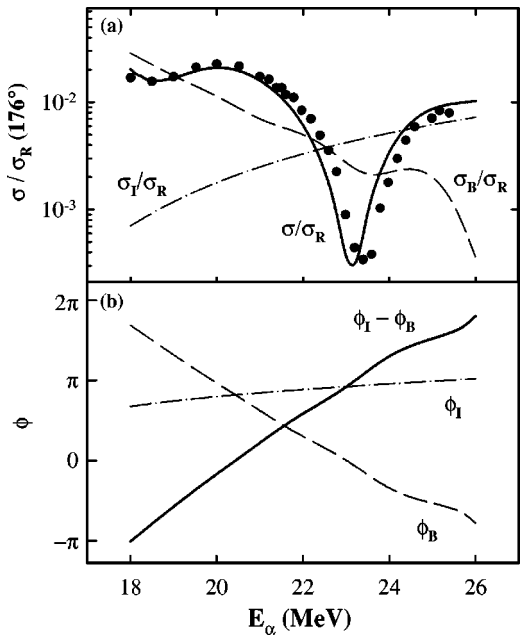

FIG. 2. (a) Experimental $^{90}\mathrm{Zr}(\alpha,\alpha_0)$ excitation function (dots) between 18 and 26 MeV [23]; predictions of the 25 MeV optical potential (full line), and barrier-internal wave contributions to the OM cross section (dashed and dash-dotted lines, respectively). (b) Phases of the barrier and internal wave contributions to the scattering amplitude (dashed and dash-dotted lines, respectively), and their difference (full line) on the same energy range.

tering on the whole angular range at 21 MeV, at 25 MeV the internal contribution becomes dominant at angles near 180°, and that—even at 21 MeV—the internal wave contribution is instrumental in the building up of the oscillations observed in the data in the backward hemisphere. The same decomposition, carried out at 40 MeV, shows that the internal contribution still dominates the data beyond about 140° at that energy.

The contributions of the barrier and internal wave components, $\sigma_B=|f_B|^2$ and $\sigma_I=|f_I|^2$, to the excitation function at 176° between 18 and 26 MeV are displayed in Fig. 2(a); the barrier wave contribution decreases steadily in this energy range, while the internal wave contribution displays the opposite behavior. In fact, the dip observed in the experimental data is seen to occur not far from the energy where the two contributions become comparable. To better understand how this dip builds up, we have plotted the phases of the the two contributions at 176°, $\phi_B=\arg(f_B)$ and $\phi_I=\arg(f_I)$, as a function of incident energy [Fig. 2(b)], as well as their difference. One sees that the latter, as a result of the steady decrease (increase) of the phase of the barrier (internal) contribution (an effect discussed by Brink and Takigawa [19]), increases rapidly with energy. Each time this difference is an odd multiple of π, the two amplitudes interfere destructively; this is the case, e.g., around 18.5 and 23.5 MeV. At 18.5 MeV the dip due to this interference is however weak, since the magnitudes of the internal and barrier wave contributions are very dissimilar; in contrast, around 23.5 MeV these magnitudes turn out to be comparable and the dip due to the interference is much more spectacular. Similarly the broad maxima observed in the excitation function around 20 and 26 MeV are due to a constructive interference between the two amplitudes whose phases differ by an integral multiple of π at these energies.

It is worth stressing that the same interpretation for the occurence of the dip observed in the experimental data consistently emerges from the barrier-internal wave decomposition of the scattering amplitude, whatever potential is used for performing this decomposition, provided this potential reproduces successfully the data; for example, the crude four-parameter Woods-Saxon potential of Wit *et al.* [23], despite its imperfections at small angles, provides the same picture for the scattering mechanism. We can therefore conclude that the existence of a substantial internal contribution to the scattering at large angles is an essential ingredient to a quantitative description of the $^{90}\mathrm{Zr}(\alpha,\alpha_0)$ data at low energy, a somewhat surprising result for a system which one would have expected to be dominated by strong absorption. As a result of this interference, which persists beyond 40 MeV incident energy, the full elastic scattering cross section is a very sensitive function of the optical model parameters, which are thus much better determined than in a strong absorption context. Another consequence of this sensitivity is that it is not straightforward to obtain a detailed reproduction of the data in the interference region.

In view of the relatively weak energy dependence of the potential expected from the microscopic approaches for

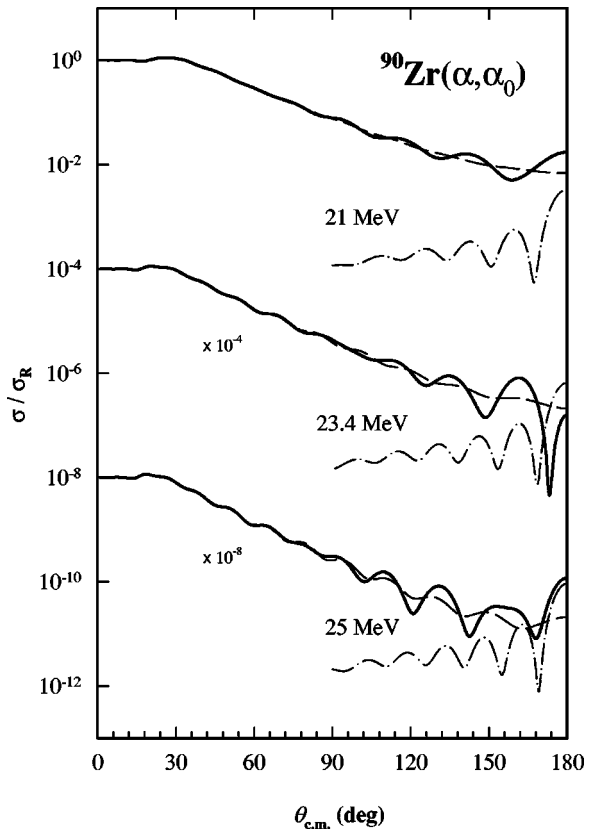

FIG. 3. Decomposition of the OM angular distributions at 21, 23.4, and 25 MeV (full line) into their barrier (dashed line) and internal-wave (dash-dotted line) contributions.

lighter systems [13] (and confirmed for lower mass targets such as ^{16}O or ^{40}Ca [8]), it is not unreasonable to calculate the location and properties of the bound and quasibound states supported by this potential around the threshold. In the calculations reported here, the lowest states allowed by the Pauli principle are taken as corresponding to $N=16$, which complements the sequence $N=4,8$, and 12 used for the closed-shell targets α, ^{16}O, and ^{40}Ca, respectively. Like for the $\alpha+^{16}$O and $\alpha+^{40}$Ca systems [8], the first allowed states are found to group into a quasirotational even-parity band, with spins ranging from 0 to N, whose bandhead falls a few MeV below the α threshold. A small renormalization of the real potential depth, performed by finely tuning the parameter α to the value 4.3675, brings the $N=16$ [26], $l=0$ state in agreement with the ^{94}Mo ground state (this value of α corresponds to a volume integral $j_V=329.1$ MeV fm^3). A comparison of the experimental values [27] with the spectrum obtained in this way appears in Table I; as in similar calculations for this system [4,5], the spectrum is too compressed at low spin, but the average experimental spacing is well reproduced (one should recall in this respect that microscopic calculations indicate that the local potential equivalent to the RGM nonlocal interaction is only approximately l independent, and that in addition the magnitude of this l dependence varies with incident energy [13].) A comparison with experiment [28] of the calculated electric quadrupole transition rates between the first states of this band also appears in Table I; one sees that the calculated $B(E2)$ values, which are obtained without any effective charge, are of the right order of magnitude, a remarkable result if one takes into account the fact that the most elaborate shell-model calculations fall short of the experimental values, even after introducing a substantial effective charge [29]. Our local potential supports also bands with higher N values which will be discussed elsewhere.

TABLE I. Excitation energies E_x and transition probabilities $B(E2)$ for the ^{94}Mo ground state band (energies in MeV, transition probabilities in e^2 fm^4).

J^π	E_x		$B(E2)(J\rightarrow J-2)$	
	Exp.	Calc.	Exp.	Calc.
2^+	0.87	0.24	392 ± 6	244
4^+	1.57	0.79	666 ± 100	337
6^+	2.42	1.64		347
8^+	2.96	2.78		328
10^+	3.90	4.18		290

In conclusion, we have shown that the low energy ($E_\alpha \simeq 25$ MeV) $\alpha-^{90}$Zr interaction is more transparent than expected, and that the interplay between the barrier and internal wave contributions to the elastic scattering amplitude is responsible for the remarkable structure observed in the elastic scattering excitation function around 180° at 23.4 MeV. This transparency makes possible the extraction of an optical potential reproducing these data, whose real part is in line with higher energy results, and in particular which belongs to the family describing the experimental data at energies where rainbow scattering sets in. This potential supports several rotational bands; the bandhead of the first (positive parity) band allowed by the Pauli principle, which corresponds to $N=16$, falls automatically near the $\alpha-^{90}$Zr threshold, and the predicted electromagnetic properties of the first states of the band—which are notoriously difficult to reproduce in shell-model calculations—are in good semiquantitative agreement with those of the ground state band in ^{94}Mo. These results strongly support the suggestion that α-clustering might still be an essential ingredient for quantitatively understanding the properties of nuclei in the $A=90$ region.

S.O. was supported by the Japan Society for the Promotion of Science.

[1] See, for example, Y. Abe *et al.*, Suppl. Prog. Theor. Phys. **68**, 1 (1980).

[2] P. E. Hodgson, in *Proceedings of the Fifth International Conference on Clustering Aspects in Nuclear and Subnuclear Systems*, Kyoto, 1988, edited by K. Ikeda, K. Katori, and Y. Suzuki [J. Phys. Soc. Jpn. **58**, 755 (1989)].

[3] M. Fujiwara *et al.*, Prog. Theor. Phys. Suppl. **132**, 1 (1998).

[4] B. Buck, A. C. Merchant, and S. M. Perez, Phys. Rev. C **51**,

559 (1995).
[5] S. Ohkubo, Phys. Rev. Lett. **74**, 2176 (1995).
[6] U. Atzrott *et al.*, Phys. Rev. C **53**, 1336 (1996).
[7] F. Michel, G. Reidemeister, and S. Ohkubo, Phys. Rev. Lett. **57**, 1215 (1986).
[8] F. Michel, S. Ohkubo, and G. Reidemeister, Prog. Theor. Phys. Suppl. **132**, 7 (1998).
[9] A. A. Pilt, Phys. Lett. **73B**, 274 (1978).
[10] K. F. Pál and R. G. Lovas, Phys. Lett. **96B**, 19 (1980).
[11] B. Buck, C. B. Dover, and J. P. Vary, Phys. Rev. C **11**, 1803 (1975).
[12] F. Michel, G. Reidemeister, and S. Ohkubo, Phys. Rev. C **37**, 292 (1988).
[13] H. Horiuchi, in *Trends in Theoretical Physics*, edited by P. J. Ellis and Y. C. Tang (Addison-Wesley, Reading, MA, 1991), p. 277.
[14] T. Wada and H. Horiuchi, Phys. Rev. C **38**, 2063 (1988).
[15] S. Ohkubo, Phys. Rev. C **38**, 2377 (1988).
[16] A. C. Merchant, K. F. Pál, and P. E. Hodgson, J. Phys. G **15**, 601 (1989).
[17] G. Reidemeister, S. Ohkubo, and F. Michel, Phys. Rev. C **41**, 63 (1990).
[18] M.-E. Brandan and G. R. Satchler, Phys. Rep. **285**, 143 (1997).
[19] D. M. Brink and N. Takigawa, Nucl. Phys. **A279**, 159 (1977); D. M. Brink, *Semi-classical Methods for Nucleus-Nucleus Scattering* (Cambridge University Press, Cambridge, 1985).
[20] P. P. Singh, P. Schwandt, and G. C. Yang, Phys. Lett. **59B**, 113 (1975).
[21] L. W. Put and A. M. J. Paans, Nucl. Phys. **A291**, 93 (1977).
[22] A. M. Kobos, B. A. Brown, R. Lindsay, and G. R. Satchler, Nucl. Phys. **A425**, 205 (1984).
[23] M. Wit, J. Schiele, K. A. Eberhard, and J. P. Schiffer, Phys. Rev. C **12**, 1447 (1975).
[24] J. Albiński and F. Michel, Phys. Rev. C **25**, 213 (1982).
[25] F. Michel *et al.*, Phys. Rev. C **28**, 1904 (1983).
[26] S. Okabe, Nucl. Phys. **A247**, 87 (1984).
[27] B. Kharraja *et al.*, Phys. Rev. C **57**, 2903 (1998).
[28] J. K. Tuli, Nucl. Data Sheets **66**, 1 (1992).
[29] Chang-hua Zhang, Shun-jin Wang, and Jin-nan Gu, Phys. Rev. C **60**, 054316 (1999).